Supporting Information

"Iridium(I) Complexes with Hemilabile *N*-Heterocyclic Carbenes: Efficient and Versatile Transfer Hydrogenation Catalysts"

M. Victoria Jiménez, Javier Fernández-Tornos, Jesús J. Pérez-Torrente,* Francisco J. Modrego, Sonja Winterle, Carmen Cunchillos, Fernando J. Lahoz, and Luis A. Oro*

Departamento de Química Inorgánica, Instituto de Síntesis Química y Catálisis Homogénea, ISQCH, Universidad de Zaragoza-C.S.I.C., 50009-Zaragoza, Spain.

Table S1, **Figure S1**. Time dependence of the catalytic transfer hydrogenation of cyclohexanone using 0.1 mol % of **7** in *i*PrOH at 80 ^{o}C with KOH as base.

Table S2, **Figure S2**. Time dependence of the catalytic transfer hydrogenation of cyclohexanone using 0.1 mol % of **6** in *i*PrOH at 80 ^{o}C with KOH as base.

Table S3, **Figure S3**. Time dependence of the catalytic transfer hydrogenation of cyclohexanone using 0.1 mol % of **14** in *i*PrOH at 80 ^{o}C with KOH as base.

Table S4, **Figure S4**. Time dependence of the catalytic transfer hydrogenation of cyclohexanone using 0.04 mol % of **14** in *i*PrOH at 80 ^{o}C with KOH as base.

Table S5, **Figure S5**. Time dependence of the catalytic transfer hydrogenation of cyclohexanone using 0.02 mol % of **14** in *i*PrOH at 80 ^{o}C with KOH as base.

Table S6, **Figure S6**. Time dependence of the catalytic transfer hydrogenation of cyclohexanone using 0.01 mol % of **14** in *i*PrOH at 80 ^{o}C with KOH as base.

Table S7, **Figure S7**. Catalyst reaction order for the transfer hydrogenation of cyclohexanone with *i*PrOH at 80 ºC for catalyst **14**.

Figure S8. ESI+ (*i*PrOH) of [IrBr(cod)(MeIm(2-methoxybenzyl))] (**7**).

Figure S9. ESI+ (*i*PrOH) of [IrBr(cod)(MeIm(2-methoxybenzyl))] (**7**) plus KOH (t = 10 min).

Figure S10. MALDI-TOF MS (linear mode, ditranol as matrix, *i*PrOH) of [IrBr(cod)(MeIm(2-methoxybenzyl))] (**7**).

Figure S11. MALDI-TOF MS (linear mode, ditranol as matrix, *i*PrOH) of [IrBr(cod)(MeIm(2-methoxybenzyl))] (**7**) plus Na*i*PrO (t = 1 min).

Figure S12. Isotopic pattern for the peak at m/z 581.9 peak in the MALDI-TOF MS (linear mode, ditranol as matrix, *i*-PrOH) of [IrBr(cod)(MeIm(2-methoxybenzyl))] (**7**) plus Na*i*PrO (t = 1 min).

Figure S13. MALDI-TOF MS (linear mode, ditranol as matrix, *i*PrOH) of [IrBr(cod)(MeIm(2-methoxybenzyl))] (**7**) plus Na*i*PrO after completed reaction (t = 5 min).

Figure S14. MALDI-TOF MS (linear mode, ditranol as matrix, *i*PrOH) of [IrBr(cod)(MeIm(2-methoxybenzyl))] (**7**) plus Na*i*PrO and cyclohexanone (t = 1min).

Figure S15. MALDI-TOF MS (linear mode, ditranol as matrix, *i*PrOH) of [IrBr(cod)(MeIm(2-methoxybenzyl))] (**7**) plus Na*i*PrO and cyclohexanone after completed reaction (t = 20 min).

Computational information: Calculated data (B3LYP) for catalytic intermediates.

Determination of the pseudo-first order rate constants (k_{obs}) for the transfer hydrogenation of cyclohexanone: $$-\frac{d[\text{cyclohexanone}]}{dt} = k_{obs}[\text{cyclohexanone}]$$

[A] and $[A]_0$ represent the concentration of cyclohexanone at a specific time and t = 0, respectively.

Table S1. Kinetic study on the transfer hydrogenation of cyclohexanone with catalyst precursor **7** with a catalyst/cyclohexanone/KOH ratio of 1:1000:5

Time (min)	$[A]/[A]_0$	$\ln([A]/[A]_0)$
0	0,872509569	-0,13638166
5	0,74595374	-0,29309169
10	0,549935394	-0,59795447
15	0,485197487	-0,72319928
20	0,385825113	-0,95237109
25	0,339742851	-1,07956627
30	0,285196831	-1,2545757
35	0,229846441	-1,47034384
40	0,208009161	-1,57017316
45	0,187760309	-1,67258908
55	0,136122701	-1,99419859
65	0,097356121	-2,32937968
72	0,075120464	-2,58866227

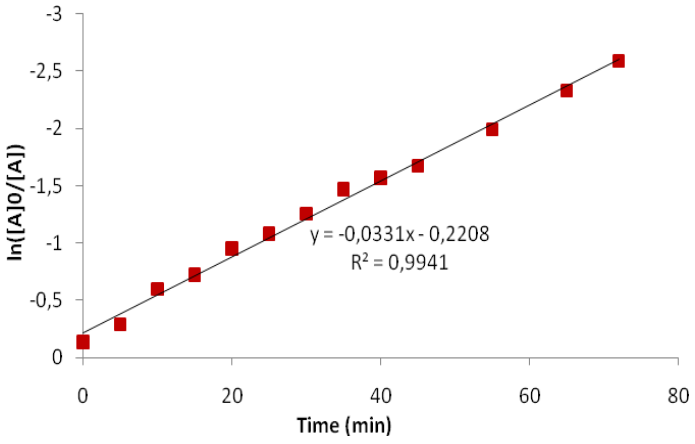

$k_{obs} = 3.31 \times 10^{-2}\ \text{min}^{-1}$

$\sigma k_{obs} = 7.68 \times 10^{-4}$

$R^2 = 0.994$

$k_{obs} = 3.31 \pm 0.08 \times 10^{-2}\ \text{min}^{-1}$

Figure S1. Time dependence of the catalytic transfer hydrogenation of cyclohexanone using 0.1 mol % of **7** in *i*PrOH at 80 ^{o}C with KOH as base.

Table S2. Kinetic study on the transfer hydrogenation of cyclohexanone with catalyst precursor **6** with a catalyst/cyclohexanone/KOH ratio of 1:1000:5

Time (min)	$[A]/[A]_0$	$\ln([A]/[A]_0)$
0	0,991803683	-0,008230091
5	0,863111616	-0,147211262
10	0,74787574	-0,290518438
15	0,642224232	-0,442817765
20	0,550517473	-0,596896583
25	0,446570652	-0,806157655
30	0,39090302	-0,93929578
35	0,357824204	-1,027713463
40	0,319628531	-1,140595799
45	0,286625388	-1,249579184
50	0,242477018	-1,416848342
55	0,222022703	-1,504975635
60	0,20199058	-1,599534218
70	0,175997033	-1,737288141
80	0,127390517	-2,060497974
90	0,112731891	-2,182742927
100	0,085188312	-2,462891038
110	0,068443089	-2,681752697

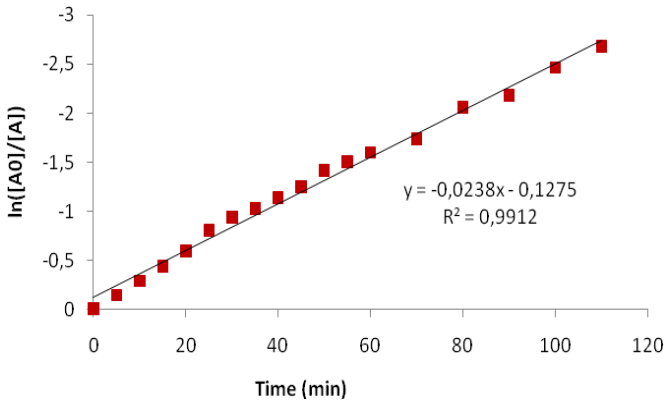

$k_{obs} = 2.38 \times 10^{-2}\ \text{min}^{-1}$

$\sigma k_{obs} = 5.60 \times 10^{-4}$

$R^2 = 0.991$

$k_{obs} = 2.38 \pm 0.06 \times 10^{-2}\ \text{min}^{-1}$

Figure S2. Time dependence of the catalytic transfer hydrogenation of cyclohexanone using 0.1 mol % of **6** in *i*PrOH at 80 ^{o}C with KOH as base.

Table S3. Kinetic study on the transfer hydrogenation of cyclohexanone with catalyst precursor **14** with a catalyst/cyclohexanone/KOH ratio of 1:1000:5

Time (min)	$[A]/[A]_0$	$\ln([A]/[A]_0)$
0	0,98140273	-0,01877237
1	0,76453984	-0,26848114
2	0,56518845	-0,51266655
3	0,4316984	-0,70261257
5	0,3316872	-1,10356292
7	0,19717493	-1,62366396
10	0,11249051	-2,17998525
11	0,09842715	-2,36589412
12	0,07526891	-2,58668816
15	0,04267942	-3,15403836
30	0,00178375	-6,32903862

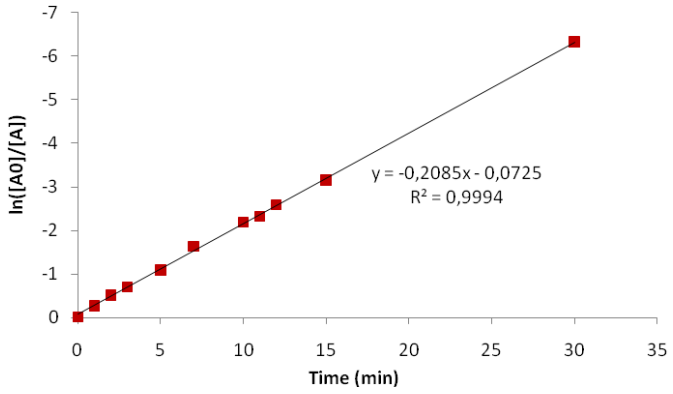

$k_{obs} = 2.08 \times 10^{-1}\,\mathrm{min}^{-1}$

$\sigma k_{obs} = 1.73 \times 10^{-3}$

$R^2 = 0.999$

$k_{obs} = 2.08 \pm 0.02 \times 10^{-1}\,\mathrm{min}^{-1}$

Figure S3. Time dependence of the catalytic transfer hydrogenation of cyclohexanone using 0.1 mol % of **14** in *i*PrOH at 80 ^{o}C with KOH as base.

Table S4. Kinetic study on the transfer hydrogenation of cyclohexanone with tcatalyst precursor **14** with a catalyst/cyclohexanone/KOH ratio of 1:2500:5

Time (min)	$[A]/[A]_0$	$\ln([A]/[A]_0)$
0	0,984002484	-0,016126858
1	0,932532036	-0,069851773
3	0,737823491	-0,304050656
5	0,547402483	-0,602570946
8	0,335438219	-1,092317486
10	0,229921076	-1,470019178
15	0,185594133	-1,684193072
20	0,140617575	-1,961711306
25	0,108088682	-2,224803257
30	0,06327641	-2,760242682
35	0,038573005	-3,255202599

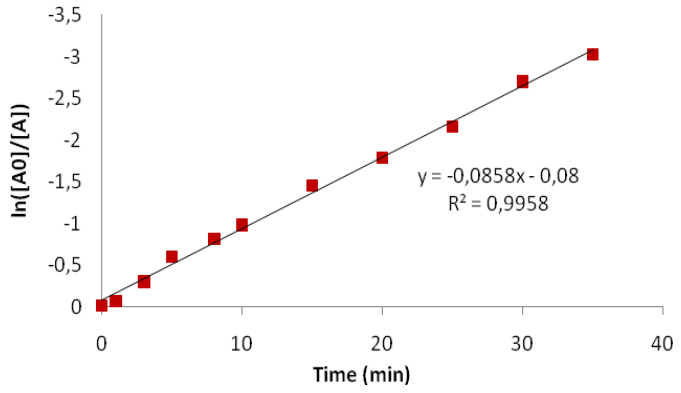

$k_{obs} = 8.58 \times 10^{-2}\ \text{min}^{-1}$

$\sigma k_{obs} = 1.86 \times 10^{-3}$

$R^2 = 0.996$

$k_{obs} = 8.60 \pm 0.02 \times 10^{-1}\ \text{min}^{-1}$

Figure S4. Time dependence of the catalytic transfer hydrogenation of cyclohexanone using 0.04 mol % of **14** in *i*PrOH at 80 ^{o}C with KOH as base.

Table S5. Kinetic study on the transfer hydrogenation of cyclohexanone with catalyst precursor **14** with a catalyst/cyclohexanone/KOH ratio of 1:5000:5

Time (min)	$[A]/[A]_0$	$\ln([A]/[A]_0)$
0	0,907832018	-0,09669592
3	0,842561517	-0,171308602
15	0,286598552	-1,249672816
55	0,150611062	-1,893054512
75	0,086233542	-2,450696063

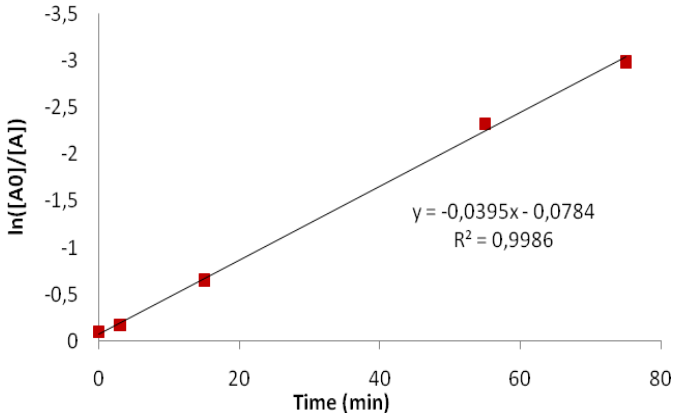

$k_{obs} = 3.95 \times 10^{-2}\ \text{min}^{-1}$

$\sigma k_{obs} = 8.54 \times 10^{-4}$

$R^2 = 0.999$

$k_{obs} = 3.95 \pm 0.08 \times 10^{-2}\ \text{min}^{-1}$

Figure S5.- Time dependence of the catalytic transfer hydrogenation of cyclohexanone using 0.02 mol % of **14** in *i*PrOH at 80 ^{o}C with KOH as base.

Table S6. Kinetic study on the transfer hydrogenation of cyclohexanone with catalyst precursor **14** with a catalyst/cyclohexanone/KOH ratio of 1:7500:5

Time (min)	$[A]/[A]_0$	$\ln([A]/[A]_0)$
0	0,97220122	-0,028192483
3	0,63693438	-0,451088645
8	0,52639579	-0,641701896
13	0,46651386	-0,762467557
23	0,35921945	-1,023821803
33	0,28085693	-1,269909901
43	0,22524716	-1,490557009
53	0,18493951	-1,687726501
63	0,14986437	-1,898024612
73	0,11792113	-2,137739249
85	0,10139571	-2,288724524
95	0,08260422	-2,493694452

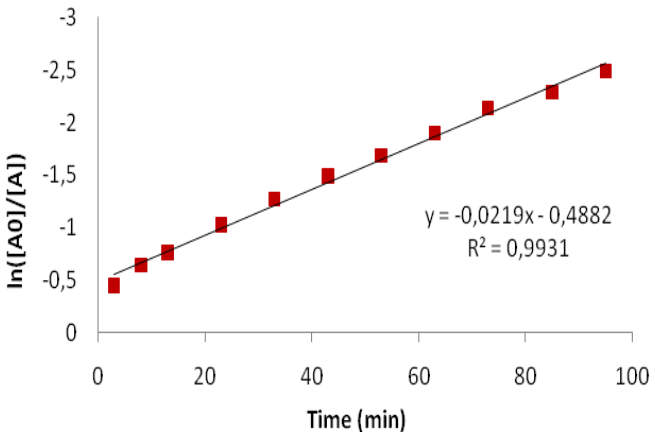

$k_{obs} = 2.19 \times 10^{-2}\ \text{min}^{-1}$

$\sigma k_{obs} = 6.10 \times 10^{-4}$

$R^2 = 0.993$

$k_{obs} = 2.19 \pm 0.06 \times 10^{-2}\ \text{min}^{-1}$

Figure S6. Time dependence of the catalytic transfer hydrogenation of cyclohexanone using 0.01 mol % of **14** in *i*PrOH at 80 ^{o}C with KOH as base.

Determination of the catalyst reaction order for the transfer hydrogenation of cyclohexanone with *i*-PrOH at 80 ºC for catalyst 14.

$$-\frac{d[\text{cyclohexanone}]}{dt} = k[\text{Ir}]^n[\text{cyclohexanone}][\text{KOH}]^m$$

$$-\frac{d[\text{cyclohexanone}]}{dt} = k_{obs}[\text{cyclohexanone}]$$

Under the experimental conditions: $k' = k[\text{KOH}]^m$ and $k_{obs} = k'[\text{Ir}]^n$ Thus,

$$\ln k_{obs} = \ln k' + n \ln[\text{Ir}]$$

Table S7. Kinetic study on transfer hydrogenation of cyclohexanone for catalyst **14** at different catalyst concentrations in *i*PrOH at 80 ºC with [cyclohexanone] = 1 mol L^{-1}.

14: cyclohexanone:KOH	[**14**] (mol L^{-1})	k_{obs} (min^{-1})	ln [Ir]	ln k_{obs}
1:1000:5	1.0 x 10^{-3}	0.2084	-6,9078	-1,5683
1:2500:5	4.0 x 10^{-4}	0.0858	-7,8241	-2,4557
1:5000:5	2.0 x 10^{-4}	0.0395	-8,5172	-3,2315
1:7500:5	1.33 x 10^{-4}	0.022	-8,9227	-3,7508

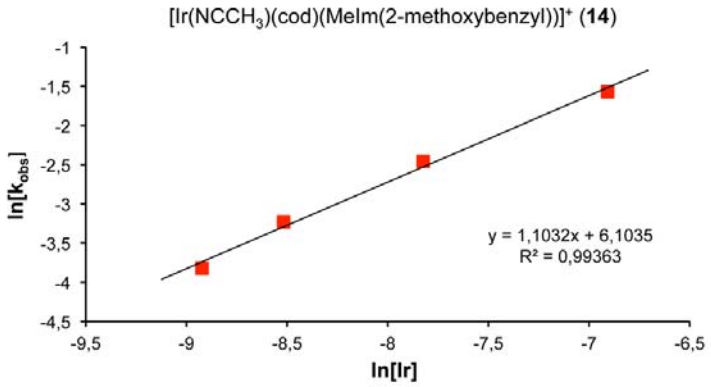

Figure S7. First order dependence on the catalyst for the transfer hydrogenation of cyclohexanone with *i*PrOH at 80 ºC for catalyst **14**.

Mass spectra ESI+ and MALDI-TOF MS (linear mode, ditranol as matrix) and simulations:

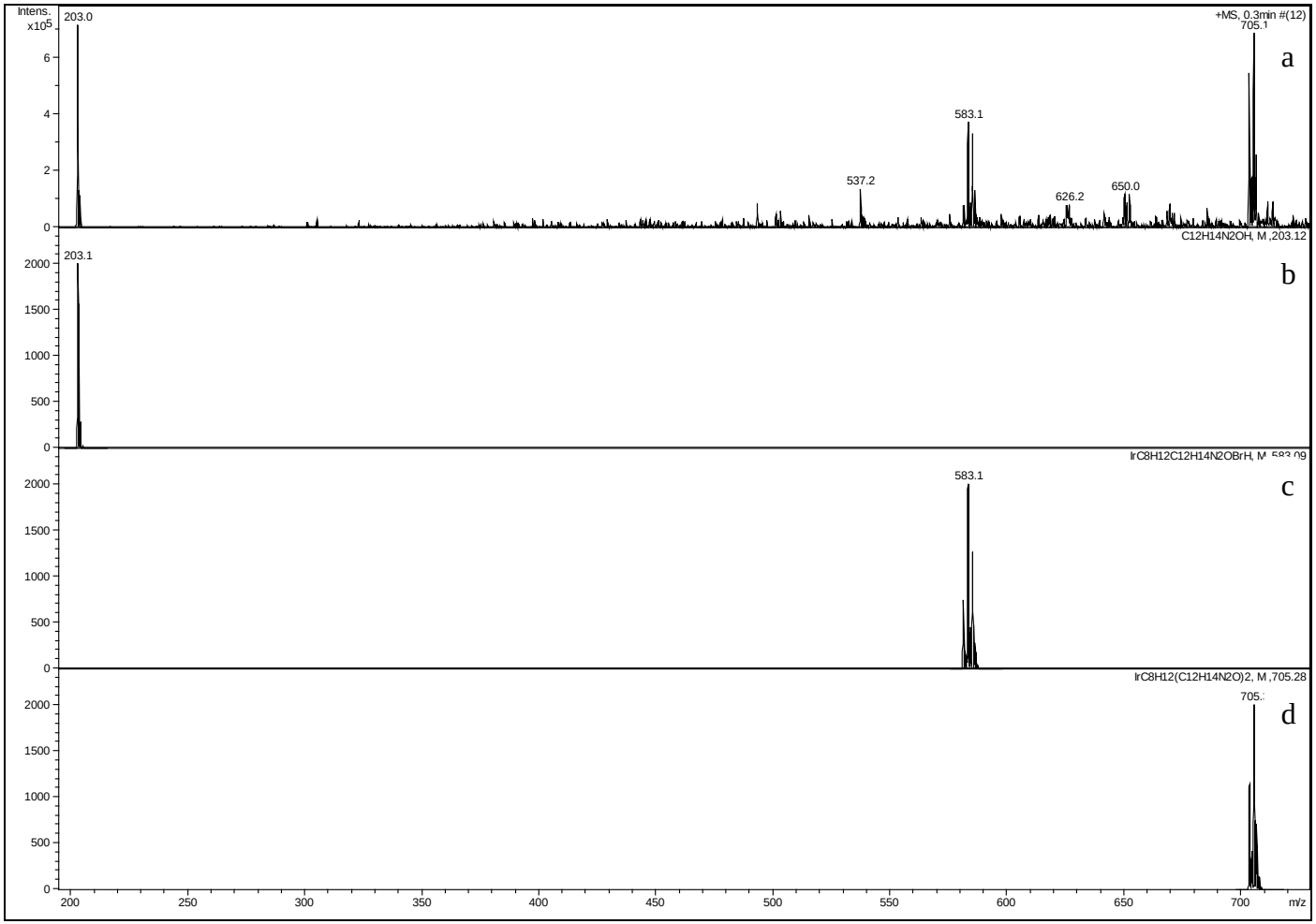

Figure S8. a) ESI+ (*i*PrOH) of [IrBr(cod)(MeIm(2-methoxybenzyl))] (**7**); b) Simulation of the peak $[MeHIm(2\text{-methoxybenzyl})]^+$ at m/z 203.1, $C_{12}H_{15}N_2O$; c) Simulation of the peak $[\mathbf{7} + H]^+$ at m/z 583.1, $IrC_{20}H_{27}N_2OBr$; d) Simulation of the peak $[Ir(cod)(MeIm(2\text{-methoxybenzyl}))_2]^+$ at m/z 705.3, $IrC_{32}H_{40}N_4O_2$.

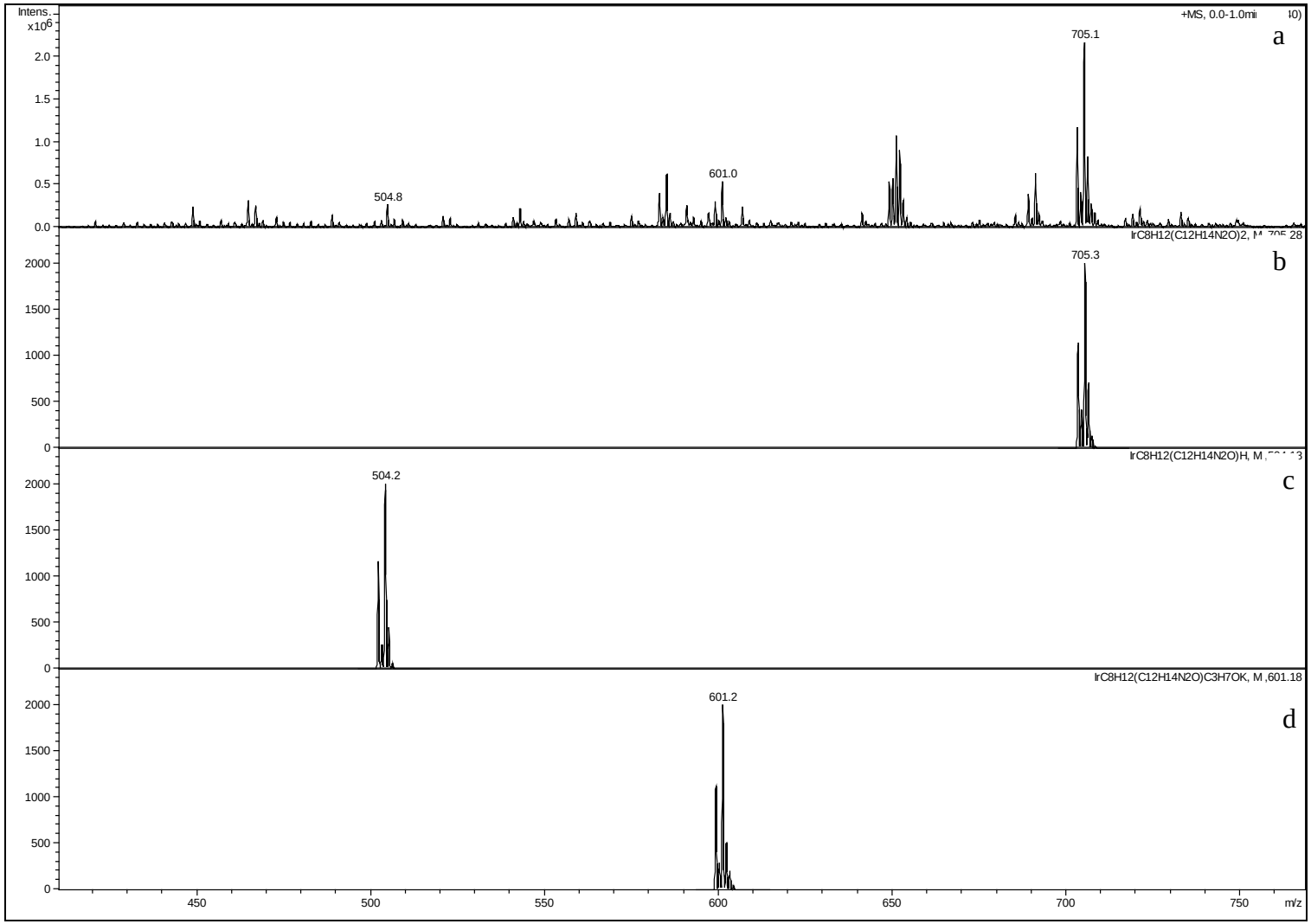

Figure S9. a) ESI+ (*i*PrOH) of [IrBr(cod)(MeIm(2-methoxybenzyl))] (**7**) plus KOH (t = 10 min); b) Simulation of the peak [Ir(cod)(MeIm(2-methoxybenzyl))$_2$]$^+$ at m/z 705.3, $IrC_{32}H_{40}N_4O_2$; c) Simulation of the peak [**7** – Br + H**]**$^+$ at m/z 504.2, $IrC_{20}H_{27}N_2O$; d) Simulation of the peak [**7** – Br + C_3H_7O + K**]**$^+$ at m/z 601.2, $IrC_{23}H_{33}N_2O_2K$.

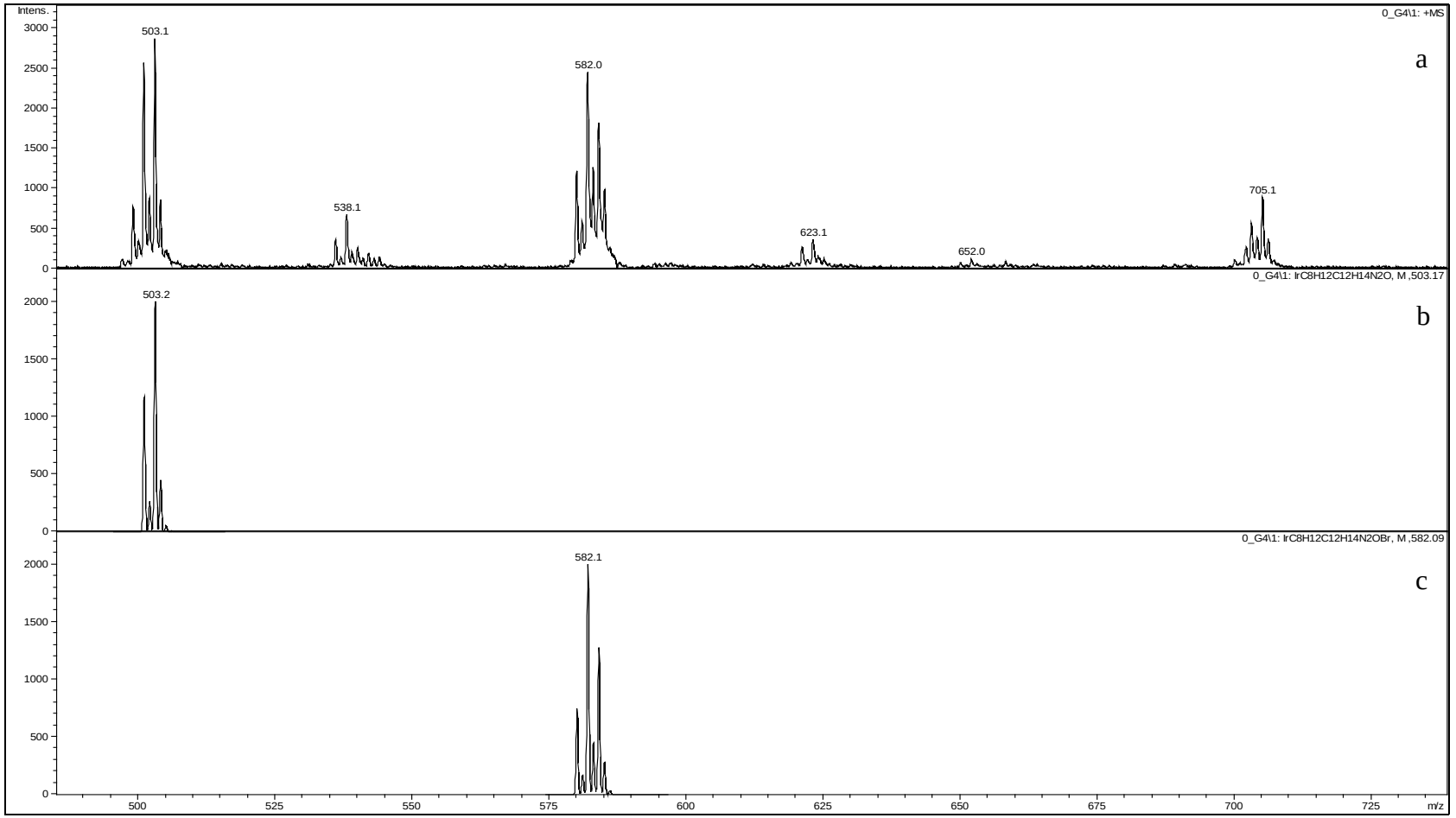

Figure S10. a) MALDI-TOF MS (linear mode, ditranol as matrix, *i*PrOH) of [IrBr(cod)(MeIm(2-methoxybenzyl))] (**7**); b) Simulation of the peak [**7** - Br]$^+$ at m/z 503.1, $IrC_{20}H_{26}N_2O$); c) Simulation of the peak [**7**]$^+$ at m/z 582.0, $IrC_{20}H_{26}N_2OBr$.

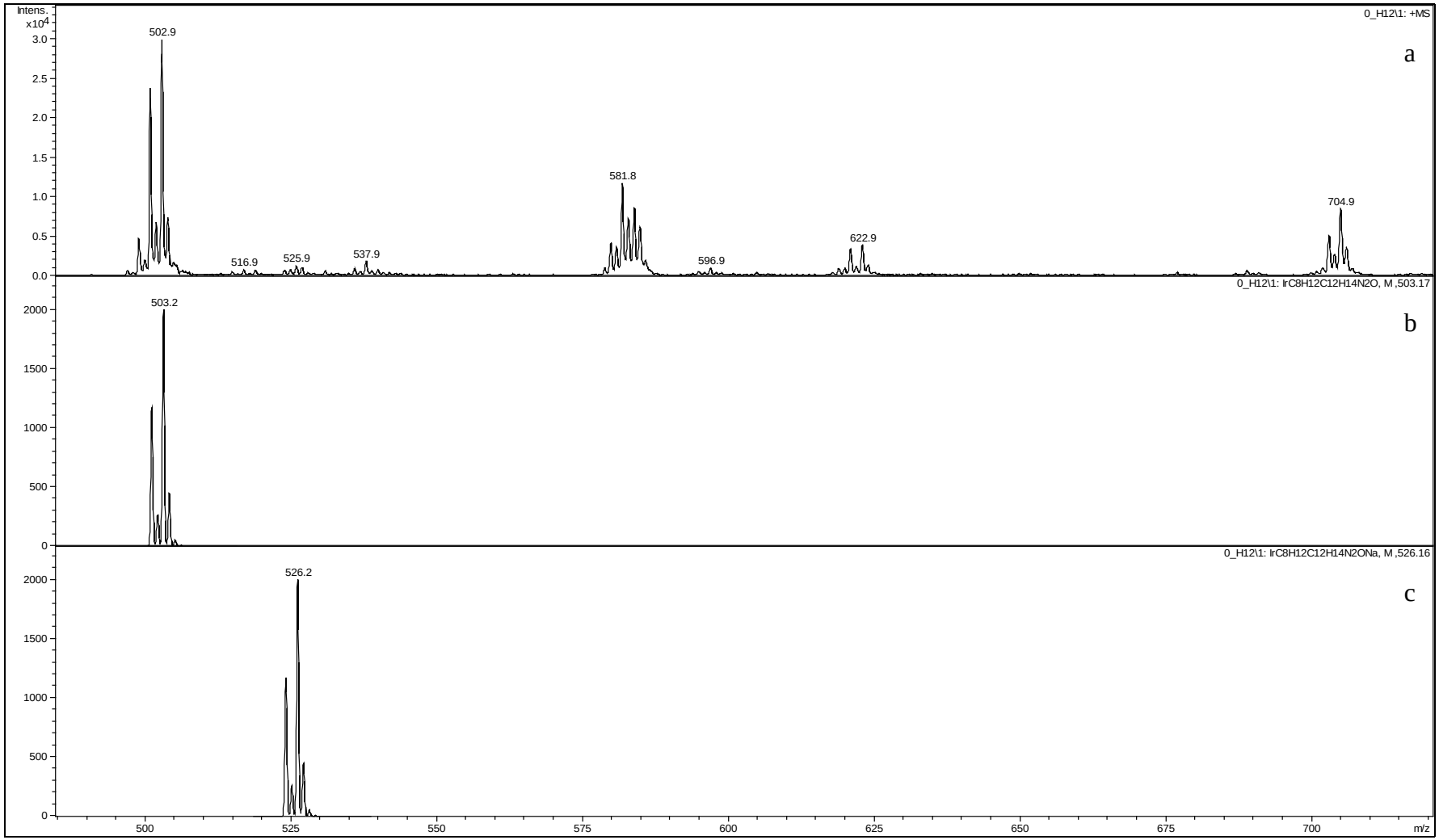

Figure S11. a) MALDI-TOF MS (linear mode, ditranol as matrix, *i*PrOH) of [IrBr(cod)(MeIm(2-methoxybenzyl))] (**7**) plus Na*i*PrO (t = 1 min); b) Simulation of the peak [**7** - Br]$^+$ at m/z 503.1, $IrC_{20}H_{26}N_2O$; c) Simulation of the peak [IrH(cod)(MeIm(2-methoxybenzyl)) + Na]$^+$ at m/z 526.6, $IrC_{20}H_{27}N_2ONa$.

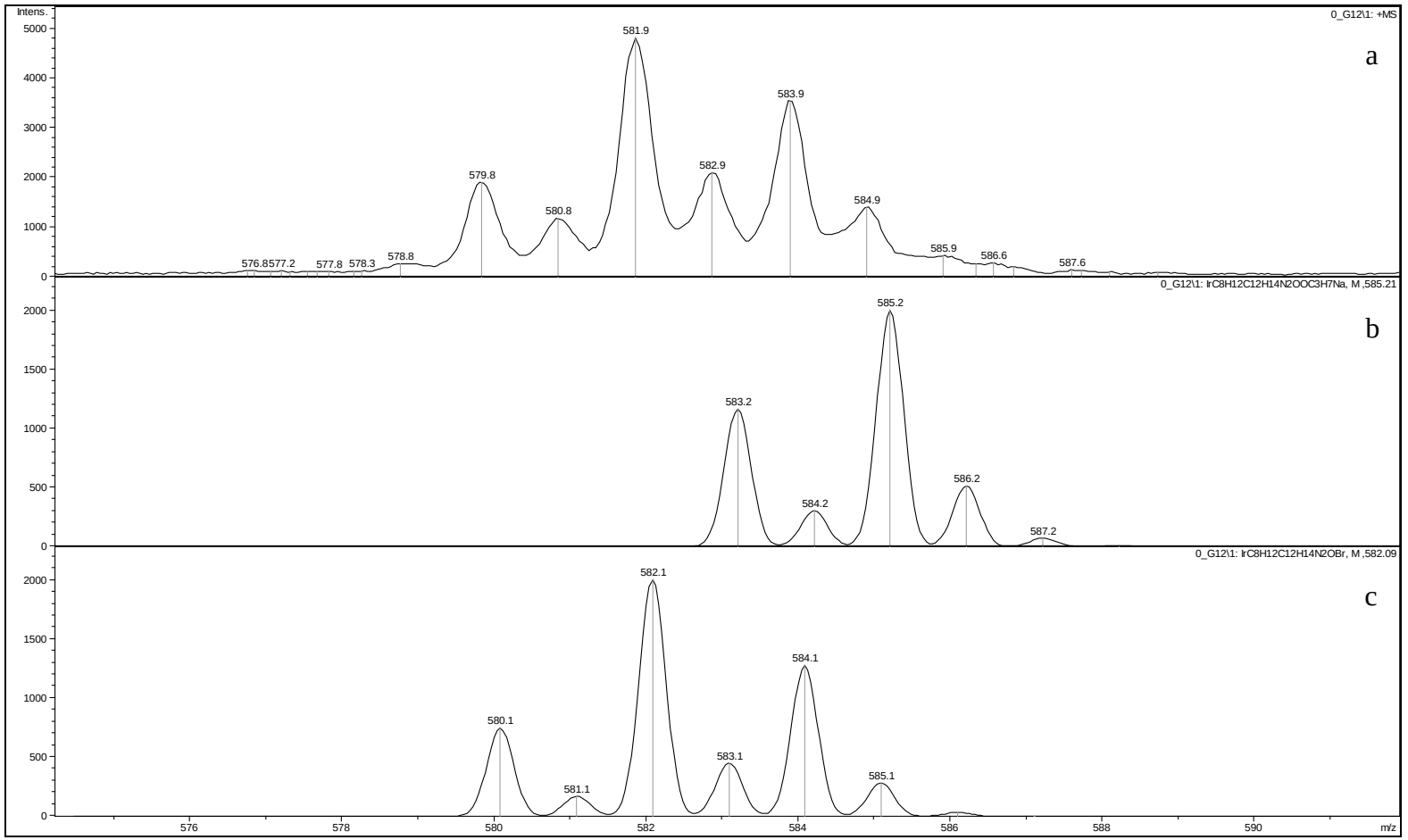

Figure S12. a) Isotopic pattern for the peak at m/z 581.9 peak in the MALDI-TOF MS (linear mode, ditranol as matrix, *i*PrOH) of [IrBr(cod)(MeIm(2-methoxybenzyl))] (**7**) plus Na*i*PrO; b) Simulation of the peak [**7** – Br + C_3H_7O + Na]$^+$ m/z 585.2, $IrC_{23}H_{33}N_2O_2Na$; c) Simulation of the peak [**7**]$^+$ m/z 582.2, $IrC_{20}H_{26}N_2OBr$.

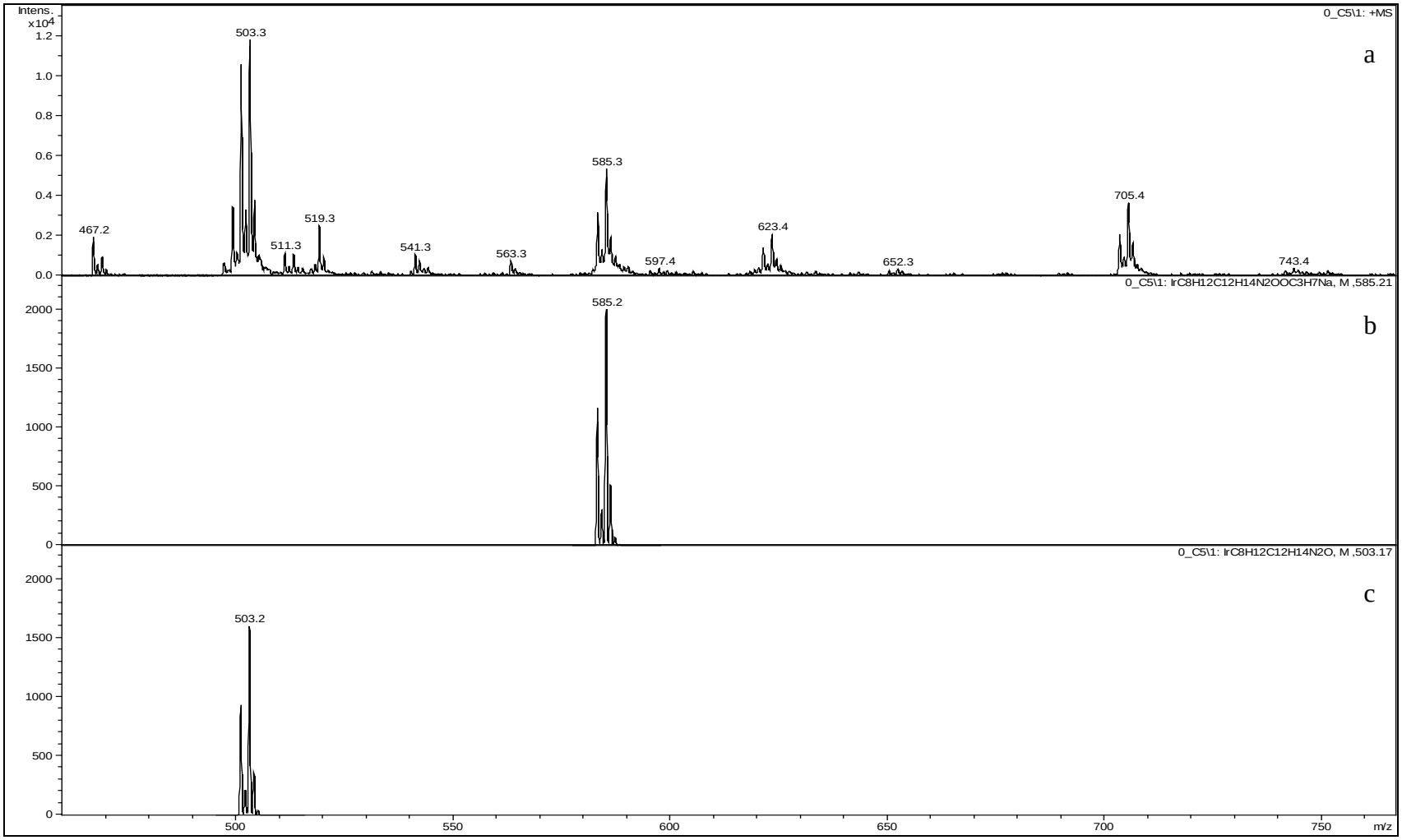

Figure S13. a) MALDI-TOF MS (linear mode, ditranol as matrix, *i*-PrOH) of [IrBr(cod)(MeIm(2-methoxybenzyl))] (**7**) plus Na*i*PrO after completed reaction (t = 5 min); b) Simulation of the peak [**7** – Br + C_3H_7O + Na]$^+$ at m/z 585.3, $IrC_{23}H_{33}N_2O_2Na$; c) Simulation of the peak [**7** - Br]$^+$ at m/z 503.1, $IrC_{20}H_{26}N_2O$.

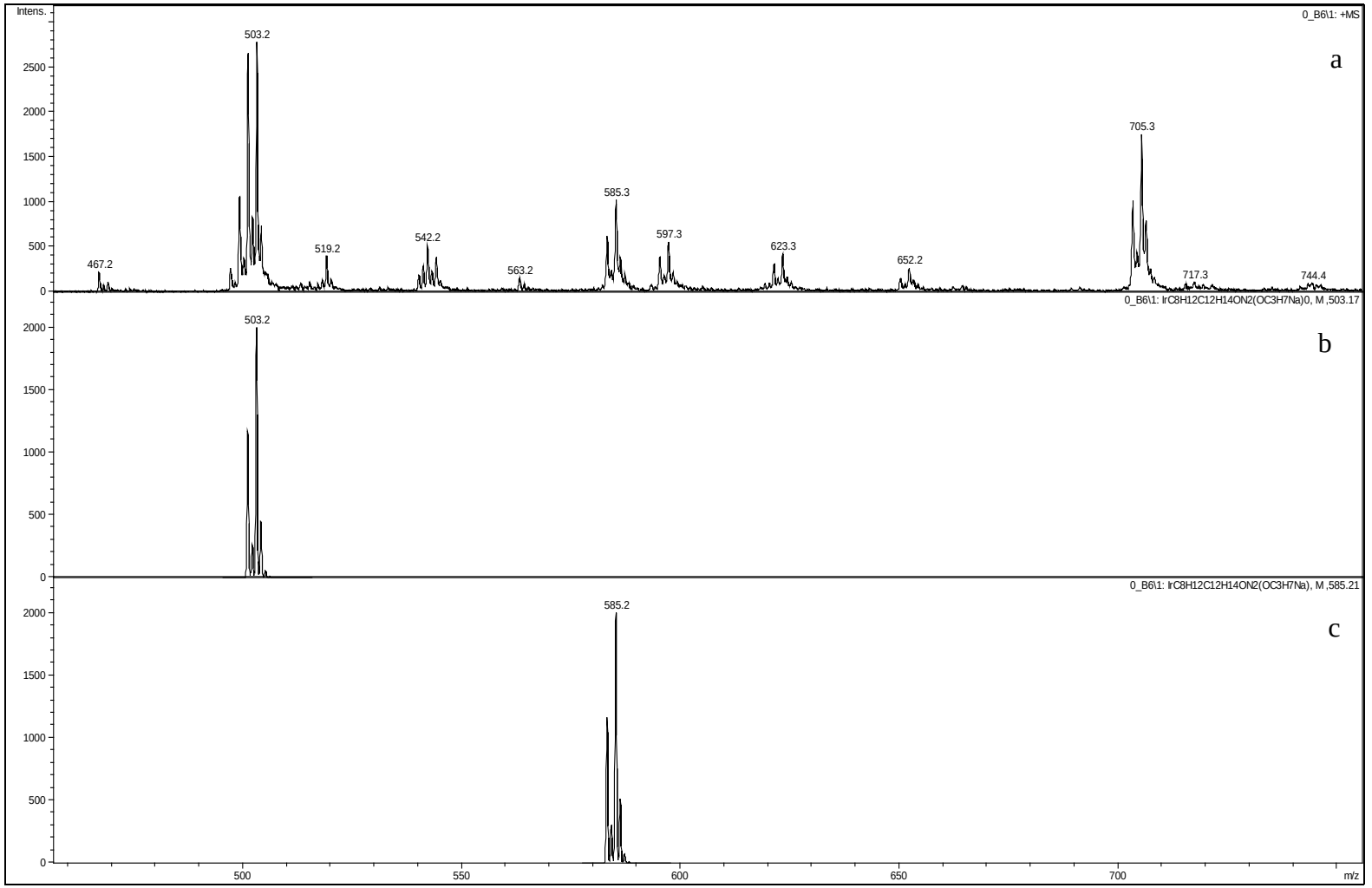

Figure S14. a) MALDI-TOF MS (linear mode, ditranol as matrix, *i*PrOH) of [IrBr(cod)(MeIm(2-methoxybenzyl))] (**7**) plus Na*i*PrO and cyclohexanone (t = 1min); b) Simulation of the peak [**7** - Br]$^+$ m/z 503.2, $IrC_{20}H_{26}N_2O$; c) Simulation of the peak [**7** – Br + C_3H_7O + Na]$^+$ at m/z 585.3, $IrC_{23}H_{33}N_2O_2Na$.

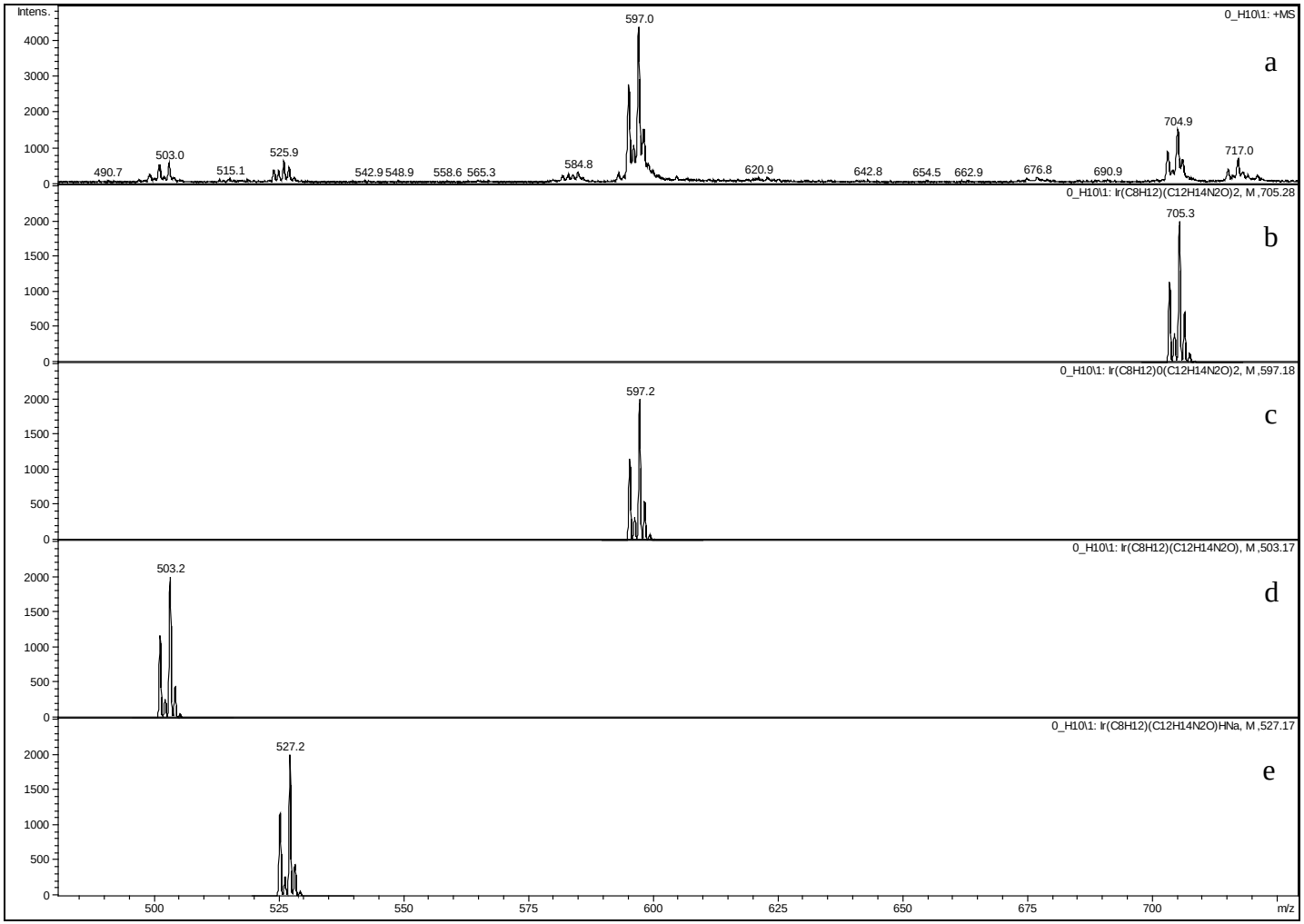

Figure S15. a) MALDI-TOF MS (linear mode, ditranol as matrix, *i*PrOH) of [IrBr(cod)(MeIm(2-methoxybenzyl))] (**7**) plus Na*i*PrO and cyclohexanone after completed reaction (t = 20 min); b) Simulation of the peak $[Ir(cod)(MeIm(2\text{-methoxybenzyl}))_2]^+$ at m/z 705.3, $IrC_{32}H_{40}N_4O_2$; c) Simulation of the peak $[Ir(MeIm(2\text{-methoxybenzyl}))_2]^+$ at m/z 597.0, $IrC_{24}H_{28}N_4O_2$; d) Simulation of the peak $[\mathbf{7} - Br]^+$ m/z 503.2, $IrC_{20}H_{26}N_2O$; e) Simulation of the peak $[IrH(cod)(MeIm(2\text{-methoxybenzyl})) + Na]^+$ at m/z 526.6, $IrC_{20}H_{27}N_2ONa$.

Computational information.

Calculated data (B3LYP) for catalytic intermediates: coordinates in Å, energies in Hartree, and graphical representation.

Compound 19a

Sum of electronic and thermal Free Energies= -1260.543416

Atom	X	Y	Z
Ir	-1.3573	-0.0184	-0.0115
N	-0.0371	-1.2693	2.4634
N	1.3579	-1.2253	0.8238
O	4.6194	-1.6718	-1.1068
C	0.0817	-0.8831	1.1585
C	1.1439	-1.8361	2.9267
H	1.2498	-2.2003	3.9364
C	2.0213	-1.8083	1.8950
H	3.0457	-2.1365	1.8228
C	-1.2155	-1.0527	3.2929
H	-0.9836	-0.3569	4.1047
H	-1.5612	-2.0008	3.7159
H	-1.9918	-0.6230	2.6595
C	1.9937	-0.9372	-0.4702
H	1.2078	-0.4993	-1.0910
H	2.3154	-1.8769	-0.9218
C	3.1628	0.0160	-0.3275
C	2.9466	1.3116	0.1499
H	1.9292	1.6014	0.4099
C	4.0057	2.2107	0.2876
H	3.8224	3.2143	0.6590
C	5.2951	1.8115	-0.0597
H	6.1281	2.5022	0.0383
C	5.5357	0.5207	-0.5360
H	6.5453	0.2267	-0.7970
C	4.4718	-0.3807	-0.6655
C	5.9084	-2.1080	-1.5058
H	6.2993	-1.5079	-2.3373
H	5.7887	-3.1416	-1.8346
H	6.6245	-2.0755	-0.6744
C	-2.6276	0.7781	-1.6776
H	-2.1362	1.6847	-2.0208
C	-3.3313	0.8511	-0.4669
H	-3.3517	1.8152	0.0383
C	-4.4288	-0.1008	-0.0241
H	-5.3680	0.1277	-0.5519
H	-4.6217	0.0968	1.0366
C	-4.0495	-1.5875	-0.1990
H	-4.3863	-1.9578	-1.1738
H	-4.5909	-2.1846	0.5435
C	-2.5442	-1.8187	-0.0386
H	-2.2853	-2.4808	0.7879
C	-1.6213	-1.8026	-1.1352
H	-0.7559	-2.4619	-1.0419
C	-1.9819	-1.5179	-2.5846
H	-2.4465	-2.3977	-3.0579
H	-1.0434	-1.3431	-3.1248
C	-2.8874	-0.2761	-2.7487
H	-2.7186	0.1684	-3.7357
H	-3.9426	-0.5685	-2.7302
O	-0.4504	1.7327	0.4980
C	-0.8157	3.0315	0.0996
C	0.0659	3.5198	-1.0610
C	-0.7071	3.9670	1.3121
H	-1.8620	3.0742	-0.2497
H	0.0009	2.8282	-1.9072
H	-0.2388	4.5163	-1.4037
H	1.1162	3.5722	-0.7541
H	-1.3610	3.6174	2.1174
H	0.3209	3.9738	1.6919
H	-0.9886	4.9960	1.0571

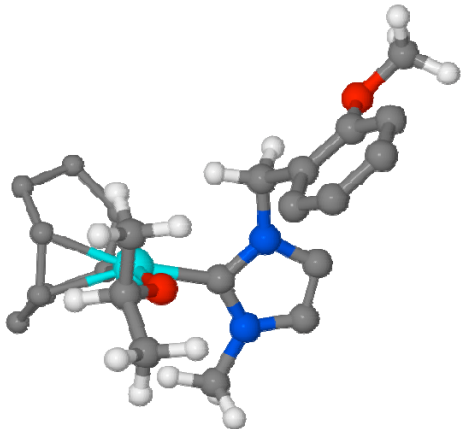

Compound 19b

Sum of electronic and thermal Free Energies= -1260.542143

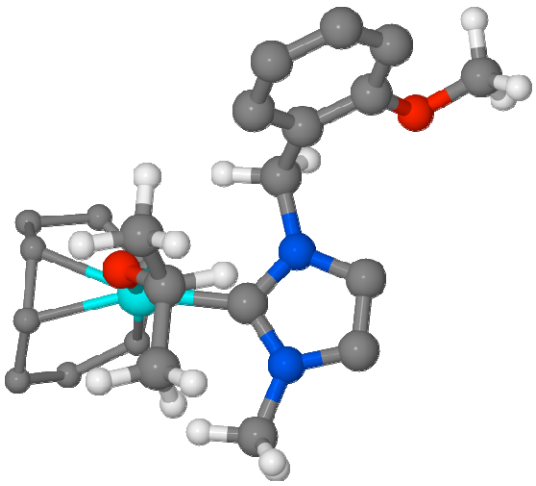

Atom	X	Y	Z
Ir	-1.4059	0.3125	-0.0214
N	0.3877	-1.5186	1.6923
N	1.3538	-1.0151	-0.1671
O	4.2613	-1.2592	-1.9607
C	0.2112	-0.7843	0.5509
C	1.6123	-2.1765	1.6835
H	1.9334	-2.8030	2.5007
C	2.2191	-1.8609	0.5144
H	3.1703	-2.1481	0.0972
C	-0.5767	-1.6182	2.7791
H	-0.1525	-1.2179	3.7047
H	-0.8619	-2.6630	2.9364
H	-1.4556	-1.0374	2.4982
C	1.6203	-0.4655	-1.5066
H	0.6926	0.0254	-1.8067
H	1.8122	-1.3040	-2.1810
C	2.7662	0.5212	-1.5544
C	2.5226	1.8847	-1.3783
H	1.5045	2.2045	-1.1717
C	3.5570	2.8204	-1.4545
H	3.3476	3.8759	-1.3138
C	4.8538	2.3853	-1.7155
H	5.6686	3.1007	-1.7821
C	5.1259	1.0262	-1.8953
H	6.1416	0.7066	-2.0956
C	4.0855	0.0956	-1.8104
C	5.5429	-1.7357	-2.3454
H	5.8661	-1.2951	-3.2965
H	5.4399	-2.8154	-2.4650
H	6.2998	-1.5285	-1.5784
C	-2.8919	1.4880	-1.2241
H	-2.3717	2.4238	-1.4139
C	-3.3925	1.3055	0.0675
H	-3.2283	2.1181	0.7703
C	-4.4317	0.2810	0.4819
H	-5.4411	0.6207	0.2014
H	-4.4218	0.2339	1.5769
C	-4.1593	-1.1315	-0.0853
H	-4.6716	-1.2640	-1.0448
H	-4.6014	-1.8759	0.5871
C	-2.6623	-1.4199	-0.2479
H	-2.3079	-2.2564	0.3546
C	-1.9352	-1.1770	-1.4582
H	-1.1134	-1.8644	-1.6680
C	-2.5100	-0.5503	-2.7202
H	-3.0903	-1.2861	-3.2997
H	-1.6630	-0.2661	-3.3572
C	-3.3668	0.7082	-2.4445
H	-3.3366	1.3646	-3.3213
H	-4.4180	0.4297	-2.3169
O	-0.7005	2.0995	0.6171
C	0.2872	2.3573	1.5800
C	-0.2632	2.1978	3.0065
C	0.7985	3.7913	1.3753
H	1.1460	1.6677	1.4681
H	-0.6474	1.1856	3.1589
H	0.5058	2.3963	3.7636
H	-1.0927	2.8965	3.1661
H	1.1997	3.9214	0.3664
H	-0.0280	4.4997	1.4999
H	1.5863	4.0451	2.0947

Compound 19c

Sum of electronic and thermal Free Energies= -1260.541866

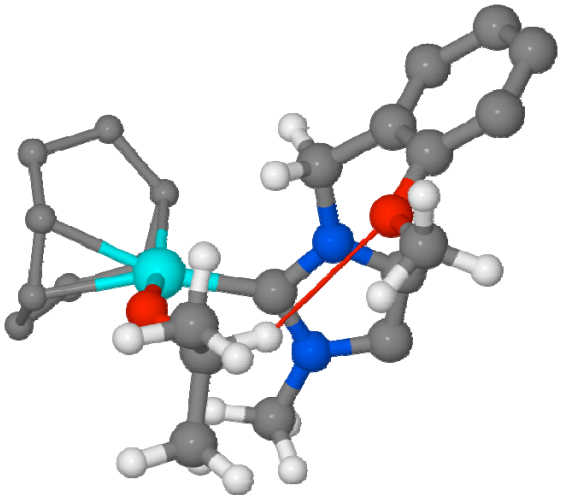

Atom	X	Y	Z
Ir	-1.5793	0.3237	0.1623
N	0.2927	-1.7527	1.4446
N	1.3070	-0.6509	-0.1072
O	3.3444	1.7472	0.3828
C	0.1082	-0.7373	0.5470
C	1.5736	-2.2814	1.3469
H	1.9141	-3.0870	1.9779
C	2.2089	-1.5924	0.3678
H	3.2079	-1.6810	-0.0246
C	-0.7016	-2.1978	2.4116
H	-0.3439	-2.0252	3.4314
H	-0.9103	-3.2637	2.2790
H	-1.6104	-1.6200	2.2403
C	1.5602	0.3254	-1.1876
H	1.1483	1.2778	-0.8474
H	0.9904	0.0141	-2.0671
C	3.0181	0.4591	-1.5524
C	3.5204	-0.1232	-2.7174
H	2.8420	-0.6924	-3.3483
C	4.8608	0.0166	-3.0871
H	5.2278	-0.4428	-3.9992
C	5.7142	0.7561	-2.2726
H	6.7590	0.8781	-2.5439
C	5.2418	1.3531	-1.1004
H	5.9207	1.9275	-0.4818
C	3.8980	1.2070	-0.7377
C	4.1583	2.5460	1.2311
H	4.9859	1.9644	1.6562
H	3.5041	2.8885	2.0324
H	4.5634	3.4141	0.6967
C	-3.1391	1.6255	-0.7954
H	-2.7091	2.6212	-0.7204
C	-3.6573	1.0799	0.3819
H	-3.5991	1.7013	1.2719
C	-4.5990	-0.1065	0.4712
H	-5.6288	0.1994	0.2285
H	-4.6175	-0.4269	1.5192
C	-4.1667	-1.3002	-0.4120
H	-4.6343	-1.2337	-1.4009
H	-4.5510	-2.2266	0.0305
C	-2.6437	-1.4012	-0.5583
H	-2.2268	-2.3313	-0.1716
C	-1.9069	-0.7905	-1.6268
H	-1.0153	-1.3288	-1.9559
C	-2.5025	0.0770	-2.7259
H	-2.9831	-0.5384	-3.5034
H	-1.6700	0.5929	-3.2205
C	-3.4949	1.1382	-2.1949
H	-3.5085	1.9947	-2.8782
H	-4.5142	0.7383	-2.1977
O	-1.0814	1.9271	1.2724
C	-0.0247	2.0672	2.1842
C	-0.4864	1.7120	3.6062
C	0.4783	3.5166	2.1169
H	0.8218	1.4056	1.9263
H	-0.8483	0.6792	3.6401
H	0.3231	1.8204	4.3394
H	-1.3138	2.3657	3.9054
H	0.8480	3.7425	1.1119
H	-0.3435	4.2065	2.3384
H	1.2849	3.7026	2.8381

Compound 19'

Sum of electronic and thermal Free Energies= -1260.501099

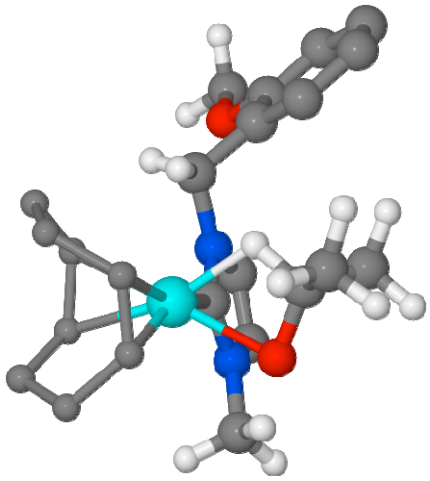

Atom	X	Y	Z
Ir	-1.4573	0.4072	0.1375
N	0.3103	-1.3671	1.8629
N	1.3576	-0.9380	0.0266
O	4.2523	-1.5540	-1.6549
C	0.1905	-0.6747	0.6944
C	1.5135	-2.0525	1.9174
H	1.7891	-2.6593	2.7652
C	2.1749	-1.7841	0.7650
H	3.1350	-2.1041	0.3968
C	-0.6931	-1.3698	2.9296
H	-0.2113	-1.7037	3.8514
H	-1.5110	-2.0516	2.6813
H	-1.0670	-0.3487	3.0347
C	1.7324	-0.3917	-1.2908
H	0.8954	0.2346	-1.5970
H	1.8208	-1.2273	-1.9902
C	3.0118	0.4197	-1.2910
C	2.9666	1.8069	-1.1387
H	2.0000	2.2795	-0.9906
C	4.1245	2.5863	-1.1799
H	4.0627	3.6629	-1.0580
C	5.3540	1.9669	-1.3882
H	6.2653	2.5567	-1.4271
C	5.4318	0.5818	-1.5548
H	6.3964	0.1172	-1.7201
C	4.2661	-0.1896	-1.5054
C	5.4615	-2.2108	-2.0106
H	5.8683	-1.8192	-2.9507
H	5.2050	-3.2635	-2.1386
H	6.2202	-2.1176	-1.2236
C	-3.0489	1.6323	-0.9100
H	-2.7047	2.6615	-0.8459
C	-3.5754	1.0635	0.2541
H	-3.5824	1.6732	1.1539
C	-4.4581	-0.1712	0.3006
H	-5.4867	0.0815	-0.0009
H	-4.5153	-0.4868	1.3479
C	-3.9079	-1.3377	-0.5476
H	-4.3321	-1.3178	-1.5583
H	-4.2373	-2.2866	-0.1088
C	-2.3747	-1.3160	-0.6250
H	-1.9198	-2.2328	-0.2479
C	-1.6311	-0.6532	-1.6902
H	-0.7377	-1.1859	-2.0200
C	-2.2730	0.1349	-2.8232
H	-2.7012	-0.5292	-3.5916
H	-1.4751	0.6987	-3.3237
C	-3.3417	1.1288	-2.3193
H	-3.3986	1.9867	-2.9989
H	-4.3336	0.6658	-2.3420
O	-1.3095	1.4688	2.0682
C	-0.5164	2.3586	1.3727
C	0.9202	2.4233	1.9133
C	-1.1287	3.7646	1.2823
H	-0.4348	1.9593	0.2529
H	1.3881	1.4366	1.9060
H	1.5542	3.1162	1.3480
H	0.8762	2.7691	2.9528
H	-2.1531	3.7256	0.9052
H	-1.1652	4.1934	2.2906
H	-0.5410	4.4349	0.6433

Compound 21
Sum of electronic and thermal Free Energies= -1067.445087

Acetone
Sum of electronic and thermal Free Energies= -193.108732

Atom	X	Y	Z
Ir	-2.6573	-0.0967	-0.3399
N	-0.9051	-0.7323	2.1023
N	0.2905	0.0901	0.5100
O	3.3526	1.4477	-0.3602
C	-0.9966	-0.2532	0.8235
C	0.4045	-0.6770	2.5696
H	0.6767	-1.0127	3.5579
C	1.1560	-0.1592	1.5691
H	2.2096	0.0572	1.5005
C	-2.0406	-1.1897	2.8890
H	-2.1502	-0.5783	3.7902
H	-1.9127	-2.2377	3.1785
H	-2.9327	-1.0841	2.2690
C	0.6841	0.7313	-0.7524
H	-0.2018	0.6793	-1.3903
H	1.4856	0.1420	-1.2043
C	1.1178	2.1722	-0.5813
C	0.1731	3.2009	-0.6048
H	-0.8742	2.9365	-0.7268
C	0.5538	4.5374	-0.4654
H	-0.1957	5.3223	-0.4868
C	1.9012	4.8510	-0.3048
H	2.2144	5.8861	-0.2008
C	2.8674	3.8417	-0.2732
H	3.9104	4.1044	-0.1423
C	2.4761	2.5052	-0.4033
C	4.7437	1.7249	-0.2981
H	5.0719	2.3301	-1.1522
H	5.2459	0.7566	-0.3288
H	5.0138	2.2414	0.6318
C	-4.0699	0.3002	-2.0111
H	-4.0139	1.3706	-2.1952
C	-4.7875	-0.1088	-0.8750
H	-5.2563	0.6719	-0.2786
C	-5.3603	-1.4940	-0.6417
H	-6.3127	-1.6179	-1.1819
H	-5.6062	-1.5676	0.4243
C	-4.3876	-2.6423	-1.0098
H	-4.5262	-2.9341	-2.0563
H	-4.6496	-3.5285	-0.4205
C	-2.9248	-2.2903	-0.7582
H	-2.4506	-2.8420	0.0517
C	-2.0673	-1.7293	-1.7227
H	-1.0010	-1.9192	-1.5982
C	-2.4593	-1.3446	-3.1376
H	-2.4842	-2.2314	-3.7913
H	-1.6646	-0.7013	-3.5343
C	-3.8051	-0.5848	-3.2259
H	-3.8011	0.0384	-4.1273
H	-4.6310	-1.2915	-3.3589
H	-2.8580	1.4201	0.2432